Stochastic Response of Beams Equipped with Tuned Mass Dampers, considering Spring Inertial Effects, Subjected to Poissonian Loads

I. P. Dunn[1], A. Di Matteo[1], G. Failla[2], and A. Pirrotta[1]
1) Dipartimento di Ingegneria, Università degli Studi di Palermo, Palermo, 90128, Italy; IainPeter.Dunn@unipa.it, Alberto.dimatteo@unipa.it, Antonina.Pirrotta@unipa.it
2) Dipartimento di Ingegneria Civile, dell'Energia, dell'Ambiente e dei Materiali Università degli Studi Mediterranea di Reggio Calabria, Reggio Calabria, 89124, Italy; giuseppe.failla@unirc.it

Abstract: This contribution considers the dynamic response of Euler-Bernoulli beams equipped with multiple tuned mass dampers, subjected to random moving loads following a Poissonian. The method proposed for the mathematical solution utilises the theory of generalised functions to find the response variables at the exact locations of the discontinuities, in this case, tuned mass dampers in which the distributed mass of the spring is also considered. This involves deriving exact, complex eigenvalues and eigenfunctions from a characteristic equation built as the determinant of a (4 x 4) matrix as oppose to the classical method requiring an (n+1 x n+1) for n number of attachments. This is always the case, in the proposed method, regardless of the number or type of attachments. Orthogonality conditions are then built for the eigenfunctions and then, the stochastic response of the beam under Poissonian loading is evaluated. To show the applicability and accuracy of the proposed procedure, a numerical application is presented in which a beam with multiple tuned mass dampers, acted upon by random moving loads, in the form of a filtered Poissonian process. The means and standard deviations at the midpoint are presented for various beam models fitted with different numbers of tuned mass damper attachments, these are found by employing a Monte- Carlo simulation.

Keywords: Euler-Bernoulli Beam; Poissonian Loading; Tuned Mass Damper; Modal Analysis.

1. Introduction

The Euler-Bernoulli model of slender beams is commonly used to calculate the dynamic response of rail and road bridges to any type of loading and it has been shown to provide extremely accurate results when validated by the finite element method (FEM). This paper will present an extension to the novel mathematical method used to find the response of Euler-Bernoulli beams under Poisson type loading. Dynamic analysis is a field which has been understood since the early part of the 20th century, however it was not until relatively recently that the dynamics of structures were given the importance that they deserve in the design and construction of structures. This change in tactics was necessitated by a number of engineering disasters which forced design standards to be updated and made more robust and it was facilitated thanks to advances in computer technology allowing increasingly complex problems to be modelled and solved. Significant advances in the transport industry, such as automation and the increasing interest in high speed rail projects, have again highlighted the importance of dynamic analysis in structures which can be typically modelled as a discontinuous Euler-Bernoulli beam.

Poissonian loading of the type presented in this paper considers various moving loads traversing the full span of the beam, by analysing the effects of moving loads on this mathematical bridge model, a greater understanding of the dynamic response which we can expect to see in real world applications, can be obtained.

This type of forcing action is used because beams subjected to moving loads have greater maximum deflections and maximum bending moments than beams which are subjected to static loads, the results should therefore, provide a more accurate picture of the actual stresses under which a bridge will suffer.

As bridges are which are subjected to higher dynamic forces from increasingly fast locomotives, this analysis takes on a greater importance due to the danger of the locomotive reaching the beam's critical velocity; at this velocity, serious damage to the beam can be sustained.

These high-speed rail projects, which are seen as significantly important to reducing carbon emissions by functioning as a viable alternative to short haul intercity flights, combined with the aging infrastructure which is present all over Europe posing a barrier to the implementation of these projects. Thorough analysis of current infrastructure combined with the addition of adequate damping to mitigate the effects of the increased forces, could reduce costs of these projects by removing the need for renewing and rebuilding existing infrastructure.

While most current studies focus on deterministic solutions to known loading, a number of studies consider the effect that random loading and a series of random moving loads have on the beams subjected to them. In many studies concerning the stochastic response of Euler-Bernoulli beams, the random loading applied follows a number of standard loading patterns, a Gaussian distribution (Di Paola et al., 1992), typical white noise (Pirrotta, 2005) a Poissonian distribution (Ricciardi, 1994), “constituted by a train of impulses of random amplitudes occurring at random time instants” (Di Matteo et al., 2016) giving a stochastic output due to these random elements (Bilello et al., 2002). Traffic loading (particularly considering road traffic, although this is also applicable to rail traffic) can be described as a Poissonian process as the magnitude of the forces is random as are their arrival times (Bucher and Di Paola, 2015).

Ricciardi (1994) proposed a method of modelling the forcing action as a filtered Poisson process, this is obtained by finding "the response of a linear undamped oscillator excited by a Poisson white noise process"
The dynamic response of a Euler-Bernoulli beam can only be accurately obtained by a very small number of methods, namely: computer models such as the finite element method (FEM), or the classical numerical method. These methods however each have significant drawbacks; the FEM is accurate at lower modes but as the number of modes under consideration increases so too does the percentage error in the eigenvalues and eigenfunctions obtained. This is also true as the number of spans increases, a beam with a high number of spans cannot be as effectively modelled by the FEM. The classical numerical method (CM) does not have this limitation, it provides exact eigenvalues and eigenfunctions regardless of the number of spans or the number of modes considered; the drawback with this method however is the large amount of computational time required to calculate the solution, as the number of spans increases, the complexity of the matrices contained in the solution of the CM grows and the required computing power increases exponentially.

This paper will expand on the work conducted by Adam et al. (2017) in which a novel numerical method was developed to find the response to a series of moving loads acting on a Euler-Bernoulli beam equipped with tuned mass dampers, this method can consider, as the CM does, complex eigenfunctions caused by damping elements, in this case from the tuned mass dampers, where the damping is localised at a specific point rather than distributed proportionally throughout the entire length of the beam as is often assumed. The method is then extended to consider a series of moving loads following a Poissonian distribution where they have random magnitudes and random arrival times, the results obtained should, therefore, more closely reflect the response of a road bridge subjected to normal traffic loading.

Further to this, in recent years, work has been undertaken to refine the mathematical model in the aim to obtain more accurate results which are closer to real-world systems. This refinement has taken the form of removing assumptions which are present in the mathematical models.

A TMD is most commonly modelled as a subsystem comprising of a lumped mass attached to the primary structural system by a spring and, in general, a viscous dashpot connected in parallel. In this standard model of a TMD, only three characteristics are generally considered, the spring stiffness, the damping coefficient and the magnitude of the lumped mass (Failla et al., 2019). It is generally assumed that the mass of the dashpot and spring are small enough in comparison to the total lumped mass to be negligible and as such, the inertial effects along the length of the spring, are neglected. This allows a major simplification of the problem by assuming a massless spring and only considering the inertial effects of the lumped mass.

In real-world applications however, this is not necessarily true as a lumped mass comprising of the total system weight will undoubtedly act differently from a distributed mass in dynamic analysis. As such, a number of studies were undertaken which aimed to better define the analytical model by including the effects from the spring's internal inertia. The model presented by Failla et al. (2019) is one such study which aimed to remove this assumption by considering the spring element's distributed mass and its effect on the beam-TMD system dynamics.

2. The Multi-Span Euler-Bernoulli Beam Problem

One of the simplest cases of a multi-span Euler-Bernoulli beam is a two-span beam fitted with one spring-mass attachment at the midpoint, this is a simplified model of a tuned mass damper (TMD) in which no dashpot is present to provide viscous damping. This allows the description of the proposed method without the introduction of too many terms thus, allowing the proposed model to retain a sufficient level of clarity. In this case however, the mathematical model of the simplified TMD is slightly more complex than that of the standard simplified TMD as the effect of the stiffness element's mass will also be considered. Typically, the spring is considered to be massless (Dunn et al., 2019), it should be clear, however, that the effects of the distributed mass will affect the dynamics of both the TMD and, by extension, the continuous beam itself. It should be emphasised however, that using the method proposed in this paper, any number of TMDs could be fitted at any point in the beam's span without changing the steps required to find the equation of motion (EoM), this will become clear.

Using the proposed formulation, supports, lumped masses, TMDs, and, indeed, any other attachment which does not cause localised rotation can be modelled as a shear discontinuity acting on a specific point. Shear discontinuities could otherwise be described as point forces located at the point of attachment of the TMD, this allows the EoM to take the form (Di Matteo et al., 2020)

$$EI\frac{\tilde{\partial}^4 w(x,t)}{\partial x^4}+\bar{m}\frac{\partial^2 w(x,t)}{\partial t^2}+R(x,t)=f(x,t) \tag{1}$$

where: the "tilde" represents the generalised derivative, EI is the flexural rigidity, $\bar{m}$ is the mass per unit length, $w(x,t)$ is the dynamic response of the beam in terms of the transversal displacement in the space and time domains, $R(x,t)$ is a generalised function (Biondi and Caddemi, 2007) used to account for the discontinuities present, in this case one single TMD and $f(x,t)$ is the forcing action. As the generalised function represents a single TMD, $R(x,t)$ takes the form Falsone (2002):

$$R(x,t) = -\sum_{j=1}^{N} P_j(t)\ \delta(x - x_j) \tag{2}$$

where: $P_j(t)$ is the shear reactionary force, a point load, and $\delta(x - x_j)$ is a Dirac's delta function positioning the reactionary force at x_j, the location of the TMD.

1.1. FREE VIBRATION

In free vibration, the left-hand side of the EoM is equal to zero and the EoM takes the form:

$$EI\frac{\tilde{\partial}^4 w(x,t)}{\partial x^4} + \bar{m}\frac{\partial^2 w(x,t)}{\partial t^2} + R(x,t) = 0 \tag{3}$$

At this point the separable variables approach is applied, wherein the time and space domains are considered independently:

$$w(x,t) = \psi(x)\, g(t) \tag{4}$$

where $g(t)$ can also be defined as: $\boldsymbol{g(t) = e^{i\omega t}}$

The space domain term $\psi(x)$ and the time domain term $g(t)$ are split; allowing for the solution of the beam's eigenvalues and eigenfunctions, however, the reactionary forces cannot be handled in this manner as the point force caused by the discontinuity is in the time domain only. $R(x,t)$ could easily be transferred into just the time and space domains by splitting $P_j(t)$ from $\delta(x - x_j)$, to retain the forcing term, $P_j(t)$ must be Fourier transformed (Failla, 2016) leading to the frequency dependent term:

$$P(x,\omega) = -\sum_{j=1}^{N} \varphi_j(\omega)\,\delta(x - x_j) \tag{5}$$

where $\delta(x - x_j)$ is a Dirac's delta function specifying the application point of the force as before and (Di Lorenzo et al., 2017):

$$\varphi_j(\omega) = -K_{TMD\,j}(\omega)\ \psi(x_j) \tag{6}$$

where $\psi(x_j)$ is the eigenfunction of deflection at the point x_j, and $K_{TMD\,j}(\omega)$ is the frequency dependent stiffness of the TMD given by the Fourier transform of the term in the time domain (Failla et al., 2019):

$$K_{TMD\,j}(\omega) = \sqrt{EA_{spring\ j}}\sqrt{\rho_{spring\ j}}\ \omega\left(\frac{\omega\,\mathrm{M}_{TMD\ j}\,\mathrm{Cos}\left(\frac{h_j\omega\sqrt{\rho_{spring\ j}}}{\sqrt{EA_{spring\ j}}}\right) + \sqrt{EA_{spring\ j}}\sqrt{\rho_{spring\ j}}\,\mathrm{Sin}\left(\frac{h_j\omega\sqrt{\rho_{spring\ j}}}{\sqrt{EA_{spring\ j}}}\right)}{-\sqrt{EA_{spring\ j}}\sqrt{\rho_{spring\ j}}\,\mathrm{Cos}\left(\frac{h_j\omega\sqrt{\rho_{spring\ j}}}{\sqrt{EA_{spring\ j}}}\right) + \omega\,\mathrm{M}_{TMD\ j}\,\mathrm{Sin}\left(\frac{h_j\omega\sqrt{\rho_{spring\ j}}}{\sqrt{EA_{spring\ j}}}\right)}\right) \tag{7}$$

where: $\mathrm{M}_{TMD\ j}$ is the magnitude of the lumped mass of the j[th] TMD, $\sqrt{EA_{spring\ j}}$ the spring stiffness of the j[th] TMD's spring, $\sqrt{\rho_{spring\ j}}$ is the distributed mass of the spring which forms part of the j[th] TMD, h_j is the spring length, and ω is the frequency.

3. Eigensolution

The exact modes of vibration can be found by applying the separable variables method, equation 4, allowing the transversal displacement $w(x,t)$, rotation $\theta(x,t)$, bending moment $m(x,\tau)$, and shear $Q(x,t)$, to be expressed in dimensionless form as:

$$w(x,t)=\psi(x)e^{\mathrm{i}\omega t}\ ;\ \theta(x,t)=\vartheta(x)e^{\mathrm{i}\omega t};\quad m(x,\tau)=\mu(x)e^{\mathrm{i}\omega\tau}\ ;\ Q(x,t)=\chi(x)e^{i\omega t} \tag{8}$$

This gives the four eigenfunctions of the response variables $\psi(x)$ deflection, $\vartheta(x)$ rotation, $\mu(x)$ bending moment, and $\chi(x)$ shear. These eigenfunctions are related through a derivative method where:

$$\begin{aligned}
&\vartheta(x)=\frac{\tilde{d}\psi(x)}{dx};\\
&\mu(x)=-\frac{\tilde{d}\vartheta(x)}{dx};\\
&\chi(x)=\frac{\tilde{d}\mu(x)}{dx};\\
&\frac{\tilde{d}\chi(x)}{dx}+\sum_{j=1}^{N}\varphi_j(\omega)\ \delta(x-x_j)+\sigma^2\psi(x)=0.
\end{aligned} \tag{9 a-d}$$

From these relations, the free vibration of the beam in the space domain can then be expressed in terms of the first eigenfunction:

$$\frac{\tilde{d}^4\psi(x)}{dx^4}+P(x,\omega)-\sigma^2\psi(x)=0 \tag{10}$$

where $\sigma^2=(\omega^2\overline{m}L^4)/EI$.

Eq. (7) shows that the reactionary force of the TMD attached at point x_j depends on the frequency dependent term concerning the spring stiffness, the damping coefficient and the attached mass.

In Eq. (5) the term $\varphi_j(\omega)$ representing the frequency dependent stiffness based on the TMD's parameters and the deflection at x_j is an unknown due to the presence of the eigenfunction of deflection. Therefore, the matrix approach must be applied:

$\mathbf{Y}(x)$ is a vector built from the response variables of the eigenfunctions:

$$\mathbf{Y}(x) = \left[\psi(x) \quad \vartheta(x) \quad \mu(x) \quad \chi(x)\right]^T \tag{11}$$

Failla (2014) proposed the following method to find the unknown $\varphi_j(\omega)$ in a closed form. Through the solution of a linear function of the 4×1 vector $\boldsymbol{c}$ which is constructed from the four integration constants which are found from the solution of the homogeneous equation a closed form expression can be obtained. This leads to the following closed analytical expression of $\mathbf{Y}(x)$:

$$\mathbf{Y}(x) = \tilde{\mathbf{Y}}(x)\boldsymbol{c} \tag{12}$$

where $\tilde{\mathbf{Y}}(x)$ is a 4×4 matrix given by the standard solution of a fourth order, homogeneous, Euler-Bernoulli beam equation:

$$\tilde{\mathbf{Y}}(x) = \boldsymbol{\Omega}(x) + \sum_{j=1}^{N} \mathbf{J}(x, x_j)\,\varphi_j(\omega) \tag{13}$$

where and each row represents an individual eigenfunction from the homogeneous solution: deflection, rotation, bending moment, and shear respectively for rows 1 through 4:

$$\boldsymbol{\Omega}(x) = \begin{bmatrix} \Omega_{\psi_1} & \Omega_{\psi_2} & \Omega_{\psi_3} & \Omega_{\psi_4} \\ \Omega_{\vartheta_1} & \Omega_{\vartheta_2} & \Omega_{\vartheta_3} & \Omega_{\vartheta_4} \\ \Omega_{\mu_1} & \Omega_{\mu_2} & \Omega_{\mu_3} & \Omega_{\mu_4} \\ \Omega_{\chi_1} & \Omega_{\chi_2} & \Omega_{\chi_3} & \Omega_{\chi_4} \end{bmatrix} \tag{14}$$

In the interest of clarity, the matrix $\boldsymbol{\Omega}(x)$ is expanded below to show the terms contained in the general solution of the homogeneous equation and the derivative method used to relate the eigenfunctions throughout the subsequent rows:

$$\begin{array}{llll} \Omega_{\psi_1}(x) = e^{-\sigma x} & \Omega_{\psi_2}(x) = e^{\sigma x} & \Omega_{\psi_3}(x) = \cos(\sigma x) & \Omega_{\psi_4}(x) = \sin(\sigma x) \\ \Omega_{\vartheta_1}(x) = -\sigma e^{-\sigma x} & \Omega_{\vartheta_2}(x) = \sigma e^{\sigma x} & \Omega_{\vartheta_3}(x) = -\sigma \sin(\sigma x) & \Omega_{\vartheta_4}(x) = \sigma \cos(\sigma x) \\ \Omega_{\mu_1}(x) = -\sigma^2 e^{-\sigma x} & \Omega_{\mu_2}(x) = -\sigma^2 e^{\sigma x} & \Omega_{\mu_3}(x) = \sigma^2 \cos(\sigma x) & \Omega_{\mu_4}(x) = \sigma^2 \sin(\sigma x) \\ \Omega_{\chi_1}(x) = \sigma^3 e^{-\sigma x} & \Omega_{\chi_2}(x) = -\sigma^3 e^{\sigma x} & \Omega_{\chi_3}(x) = -\sigma^3 \sin(\sigma x) & \Omega_{\chi_4}(x) = \sigma^3 \cos(\sigma x) \end{array}. \tag{15}$$

The discontinuities are considered (as shown in equation 13) through the vector $\mathbf{J}(x, x_j)$ which can be expanded as (Failla et al., 2019):

$$\mathbf{J}(x, x_j) = \left[J_{\psi}^{(p)} \quad J_{\vartheta}^{(p)} \quad J_{\mu}^{(p)} \quad J_{\chi}^{(p)} \right]^T \tag{156}$$

At this point, the boundary conditions at the extremes of the beam are enforced:

$$\mathbf{Bc} = \mathbf{0} \tag{17}$$

Where $\mathbf{B}$ is a 4 x 4matrix constructed from enforcing the boundary conditions on the matrix $\tilde{\mathbf{Y}}(x)$ and as before $\mathbf{c}$ is a 4 x 1 vector of the unknown constants.

From here, the characteristic equation can then be built as the determinant of the 4×4 matrix $\mathbf{B}$:

$$\det(\mathbf{B}) = 0 \tag{18}$$

Then, the non-trivial solutions of $\mathbf{c}$ are found and exact closed form expressions can be built for the beam's eigenfunctions. Due to the presence of a dashpot in the TMD model, localised damping will be present and therefore, the eigenfunctions will be complex as will the mode shapes.

4. Orthogonality Conditions

Following the procedure presented in Oliveto et al. (1997), the orthogonality conditions are built to derive the particular impulse response function of this beam.

Firstly the EoM in free vibration in the form shown below is considered:

$$\frac{\tilde{d}^4\psi_m(x)}{dx^4} - \sigma_m{}^2\psi_m(x) + \sum_{j=1}^{N} K_{TMD\ j}(\omega_m)\psi_m(x_j) = 0 \tag{169}$$

Considering modes m and n, multiplying the EoM at mode m by $\psi_n(x)$ and at mode n by $\psi_m(x)$ and then integrating between 0 and L with respect to x:

$$\int_0^L \frac{\tilde{d}^2\psi_m(x)}{dx^2}\frac{\tilde{d}^2\psi_n(x)}{dx^2}dx - \sigma_m{}^2\int_0^L \psi_{mn}(x)dx + \sum_{j=1}^{N} K_{TMD\,j}(\omega_m)\psi_{mn}(x_j) = 0 \tag{20}$$

where: $\psi_{mn}(x) = \psi_m(x)\psi_n(x)$

$$\int_0^L \frac{\tilde{d}^2\psi_n(x)}{dx^2}\frac{\tilde{d}^2\psi_m(x)}{dx^2}dx - \sigma_n{}^2\int_0^L \psi_{mn}(x)dx + \sum_{j=1}^{N} K_{TMD\,j}(\omega_n)\psi_{mn}(x_j) = 0 \tag{21}$$

Integrating by parts and subtracting Eq. (21) from Eq. (20) then yields the first orthogonality condition:

$$(\sigma_m{}^2 - \sigma_n{}^2)\int_0^L \psi_{nm}(x)dx + \sum_{j=1}^{N}[K_{TMD\ j}(\omega_n) - K_{TMD\ j}(\omega_m)]\psi_{nm}(x_j) = 0 \tag{22}$$

The second orthogonality condition is then found by multiplying Eq. (20) by σ_n and Eq. (21) by σ_m and then subtracting Eq. (21) from Eq. (20):

$$\sigma_{m-n}\int_0^L \frac{\partial^2\psi_{mn}(x)}{\partial x^2}dx + \sigma_m\sigma_n(\sigma_{m-n})\int_0^L \psi_{nm}(x)dx + [\sigma_m K_{TMD\ j}(\omega_n) - \sigma_n K_{TMD\ j}(\omega_m)]\psi_{nm}(x_j) = 0 \tag{23}$$

where $\frac{\partial^2\psi_{mn}(x)}{\partial x^2} = \frac{\partial^2\psi_m(x)}{\partial x^2}\frac{\partial^2\psi_n(x)}{\partial x^2}$ and $\sigma_{m-n} = (\sigma_m - \sigma_n)$

5. Forced Vibrations

These orthogonality conditions are then used to derive the beam's response to arbitrary loading. This is accomplished by using the complex modal superposition principle as defined by (Di Lorenzo et al., 2017) where the complex modal impulse response function is used. This leads to (Adam et al., 2017):

$$w(x,t)=\sum_{k=1}^{\infty}\psi_k(x)\frac{1}{i\,\Xi_k\,\omega_k}\int_0^t f(\tau)\,e^{i\omega_k(\tau-t)}d\tau \tag{24}$$

where: $f(\tau)$ is the moving load dependent term and Ξ_k is the effect that the beam's mass and the attached TMD have on the beam's response:

$$\Xi_k=2\int_0^L \bar{m}(x)\left[\psi_k(x)\right]^2 dx+\sum_{j=1}^{N} TMD_j\left[\psi_k(x_j)\right]^2 \tag{25}$$

where

$$\text{TMD}_\text{j}=\left(\frac{2\,\beta\,\text{M}_{TMD\,\text{j}}\,\omega_k\,\text{Cos}(2\alpha)+\sqrt{\beta}\,\text{Sin}(2\alpha)(-\beta+\omega_k^2\text{M}_{TMD\,\text{j}}^2)-2\,\rho_{spring\,\text{j}}\,\omega_k(EA_{spring\,\text{j}}\,\text{M}_{TMD\,\text{j}}+h_j(\beta+\omega_k^2\text{M}_{TMD\,\text{j}}))}{2\,\omega_k\left(\sqrt{\beta}\,\text{Cos}(\alpha)-\omega_k\,\text{Sin}(\alpha)\text{M}_{TMD\,\text{j}}\right)^2}\right) \tag{26}$$

where $\alpha=\left(\frac{h_j\omega_k\sqrt{\rho_{spring\,\text{j}}}}{\sqrt{EA_{spring\,\text{j}}}}\right)$ and $\beta=EA_{spring\,\text{j}}\,\rho_{spring\,\text{j}}$.

For a moving load, the response equation takes the following form:

$$w(x,t)=\sum_{k=1}^{\infty}\left(\psi_k(x)\int_0^t e^{i\omega_k(t-\tau)}d\tau\right)\frac{\int_0^L\psi_k(x)\delta(x-V_0\,\tau)\,dx}{i\,\Xi_k\,\omega_k} \tag{27}$$

where: $\delta(\cdot)$ is a Dirac's delta function and V_0 is the velocity of the load.

Further, when considering multiple loads traversing the beam, the effects of preceding loads must also be accounted for (Dunn et al., 2019):

$$w(x,t)=\sum_{k=1}^{\infty}\psi_k(x)\frac{\int_0^L\psi_k(x)\delta(x-V_0\,\tau)\,dx}{i\,\Xi_k\,\omega_k}\left(\int_{\tau_L^0}^t e^{i\omega_k(t-\tau)}d\tau-\int_{\tau_L^E}^t e^{i\omega_k(t-\tau)}d\tau\right) \tag{28}$$

where: τ_L^0 and τ_L^E denote the start and end times of the L$^{\text{th}}$ load.

Due to the presence of complex conjugate pairs, Eq. (28) can revert to the following real form (Failla et al., 2019):

$$w(x,t)=2\,\text{Re}\left[\sum_{k=1}^{\infty}\psi_k(x)\frac{\int_0^L\psi_k(x)\delta(x-V_0\,\tau)\,dx}{i\,\Xi_k\,\omega_k}\left(\int_{\tau_L^0}^t e^{i\omega_k(t-\tau)}d\tau-\int_{\tau_L^E}^t e^{i\omega_k(t-\tau)}d\tau\right)\right] \tag{29}$$

6. Poissonian Loading

A Poissonian white noise process is a type of delta-correlated process (Di Paola et al., 1995), which is "simple, robust and gives accurate results" (Di Paola and Ricciardi, 1992) when used to model loading caused by free flowing traffic, i.e. traffic unencumbered by an unusually heavy volume causing a continuous series of moving loads due to jams and tailbacks. Poissonian processes are most commonly defined as (Ricciardi, 1994):

$$S_P(t) = \sum_{P=1}^{N(t)} Y_P \delta(t - T_P) \tag{30}$$

where $N(t)$ is a counting function giving the number of impulses in the time interval (0,t), Y_P is the random amplitude (Di Paola and Pirrotta, 1999) of the forcing action, and $\delta(t - T_P)$ is a series of Dirac delta impulses Furtmüller et al. (2019) occurring at independent random times (T_P) following a Poissonian distribution.

When considering a moving load, this characterisation of the Poissonian load must be altered, it is also assumed that the loads will have a constant and equal velocity:

$$S_P(t) = \sum_{P=1}^{N(t)} Y_P \delta\left[x - \left(t - T_P\right)V_0\right] W(t - T_P, t_L) \tag{31}$$

where $\delta\left[x - \left(t - T_P\right)V_0\right]$ is a modification of the Dirac delta function from equation (30) in which moving loads arriving at random times with random amplitudes are considered, t_L is the time taken for the load to traverse the beam, length divided by the velocity of the moving load, L/V_0 and $W(t - t_p, t_L)$ is a window function which removes the force after it has traversed the beam; here $U(\cdot)$ is a unit step function: $W(t - T_P, t_L) = U(\tau)[1 - U(\tau - t_L)]$.

Following the method proposed by Ricciardi (1994), and Di Paola and Ricciardi (1992) the Poisson process is filtered to ensure that it is applicable to the beam's characteristics, this filtering causes Eq. (31) to take the following form:

$$S_k\left(t\right) = \sum_{P=1}^{N(t)} Y_P \psi_k\left(V_0\, \tau\right) W(t - T_P, t_L) \tag{32}$$

Substituting this into the original EoM gives:

$$EI\frac{\tilde{\partial}^4 w\left(x,t\right)}{\partial x^4} + \bar{m}\frac{\partial^2 w\left(x,t\right)}{\partial t^2} + R\left(x,t\right) = \sum_{\mathrm{P}=1}^{N(t)} Y_P \psi_k\left(V_0\, t\right) W\left(t - T_P, t_L\right) \tag{33}$$

Considering the theory of separable variable, this can also take the following form in the time domain:

$$\ddot{g}_k\left(t\right) + {\omega_k}^2 g_k(t) = \frac{2}{\Xi_k} S_k(t) \tag{34}$$

where $S_k(t)$ is the random forcing action at the kth mode, this takes the form:

$$S_k(t) = \sum_{P=1}^{N(t)} Y_P \psi_k(V_0 \tau) W(\tau, t_L) \tag{35}$$

7. Numerical Application

In this section a brief numerical application of the method presented in this paper. A bare beam, a beam fitted with a standard TMD and a beam fitted with a TMD in which the spring mass is considered are subjected to Poissonian loading and their mean and standard deviation responses in terms of midspan displacement are compared.

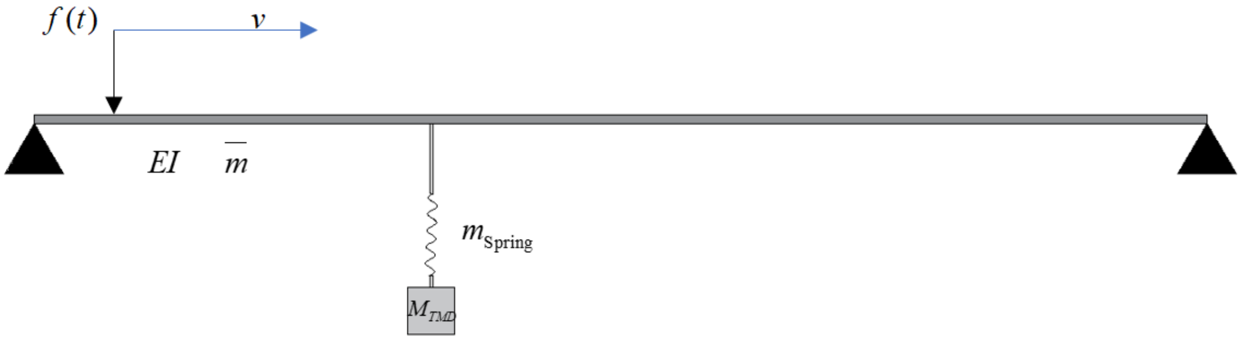

Figure 1. Euler-Bernoulli beam fitted with a TMD.

Figure 1 shows the beam configuration with one spring-mass attachment. The beam has a total length, L, of 6 m, a cross-sectional area, A, of 0.0625 m^2, the Young's modulus, E, is equal to $210\ GPa$, the second moment of area , $I = 0.000326\ m^4$, the mass per unit length $\overline{m} = 487.5\ Kg$, and the density $\rho = 7800\ kg/m^3$. The TMD tuning parameters selected for both the traditional and helical models are identical, however it should be noted that their distribution of masses will vary, both TMD models are attached at one third of the beam length, 2 m. In the traditional model the spring stiffness, k_{TMD} = 13.125 MN/m and the lumped mass, M_{TMD} = 812.5 kg were selected based on the mechanical characteristics chosen in the helical spring model in which the spring had a length, h = 1 m, stiffness, given by the Young's modulus multiplied by the cross sectional area, EA = 13.125 MN/m, a lumped mass kg and a distributed mass, m_{Spring} = 312.5 kg and the lumped mass M_{TMD} = 500 kg.

Firstly, the natural frequencies were obtained comparing the classical model of the TMD to the helical model, then a finite element model in which the mass of the spring was considered was used to validate the helical model. The results are reported below in Table 1:

Natural Frequency	FEM	Helical Spring Model	Lumped Mass Model
1st	85.978 Rad/s	85.978 Rad/s	85.976 Rad/s
2nd	360.889 Rad/s	360.888 Rad/s	360.810 Rad/s
3rd	923.942 Rad/s	923.956 Rad/s	923.956 Rad/s
4th	1453.414 Rad/s	1453.410 Rad/s	1449.149 Rad/s
5th	2351.407 Rad/s	2351.838 Rad/s	2343.061 Rad/s

As shown, the helical model is validated by the finite element model where a very good agreement is seen between both sets of natural frequencies. It is also evident that only a very small error exists between the classical TMD model and that of the helical model. It should be noted however that a general trend emerges showing that at higher frequencies, the error between the classical TMD and helical models grows.

To obtain the results from dynamic testing, a Monte-Carlo simulation was run 2000 times for each mode, 10000 times in total. The arrival rate set for these loads was 0.375 loads per second, the velocity, v, was 34 m/s, and the magnitude was between the range of 40000 and 240000 N.
The figures below show the responses obtained.

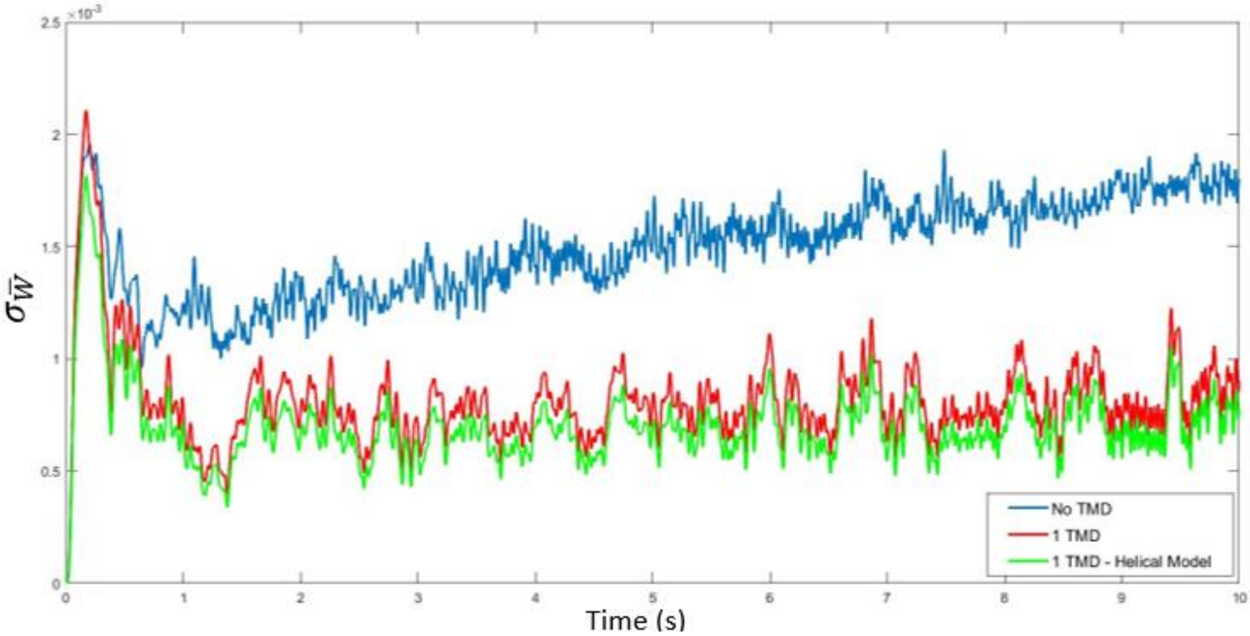

Figure 2. Standard Deviation of Displacement.

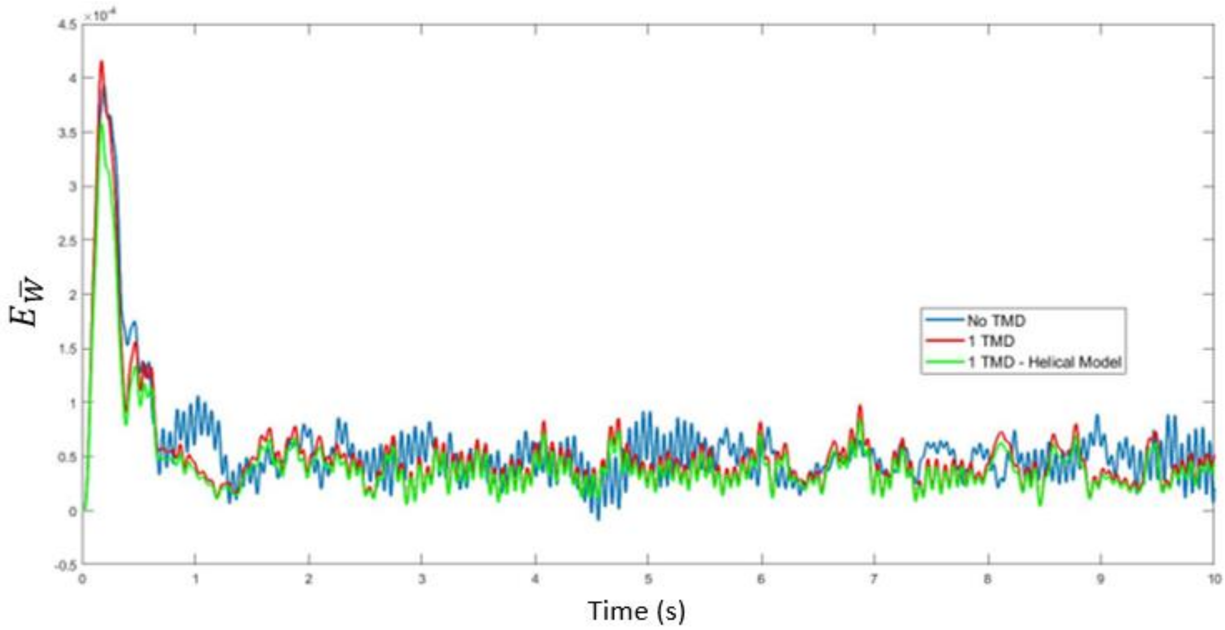

Figure 3. Mean Displacement.

Figures 2 and 3 allow two conclusive conclusions to be drawn, firstly, the traditional method used to model TMDs is highly accurate and the results obtained correlate well with those from the more complex and, therefore more accurate, helical model. The helical model does appear to slightly outperform the traditional TMD model however, the two models have very similar dynamic responses. This, correlation is observed in both the standard deviation and the mean displacement figures where the helical model and the traditional model have very similar response curves but with a slightly lower magnitude in the helical response. Secondly, it can be clearly observed that the tuning parameters selected are insufficient to provide a meaningful reduction in the mean displacement of the bridge structure, however, having observed a reduction in the standard deviation of the displacement, it is clear that some benefit is derived from the application of a TMD.

8. Conclusions

A novel method has been presented to find the response of an Euler-Bernoulli beam fitted with TMDs subjected to Poissonian loading in which the spring inertia effects are considered. This method yields a number of advantages over traditional methods, principally, a reduction in the computational power required to find an exact solution, with respect to the classical mathematical method. This was achieved by viewing an attachment, in this case a spring-mass damper with spring inertial effects, not as a discontinuity, wherein the beam would have to be split at each attachment point, considered as two separate but coupled continuous beams which are related through their boundary conditions, but rather, as a point load. By considering attachments as reactionary forces creating loading at specific points, the number of unknown constants is reduced which greatly simplifies the classical matrix method solution, as, using the proposed method, there will only ever be 4 unknown constants which must be computed as opposed to the classical case in which 4(N+1) constants for N number of attachments must be found. The use of "smart" dampers was also discussed, these are still relatively new and their application is not yet widespread. This means that this is still a market ripe for expansion and with more efficient and accurate dynamic analysis, it may be easier to promote the introduction of these novel types of dampers to existing structures. The introduction of these novel types of dampers to the proposed analytical method has also been discussed and provided that a robust mathematical method has been developed for each type of damper, this should be more than possible.

Finally, a Monte-Carlo simulation was run in which three beam configurations were subjected to Poissonian loading. The results then showed an excellent correlation between the two TMD models despite a relatively minor improvement in the reduction of the maximum displacement with respect to the bare beam. The method proposed herein is shown to be applicable to cases involving Poissonian loading and can therefore be extended to consider other cases of stochastic loadings and cases involving smart damping devices.

Acknowledgements

The research presented in this project was carried out as part of the H2020-MSCA-ETN-2016. This project has received funding from the European Union's H2020 Programme for research, technological development and demonstration under grant agreement number 721493

References

Adam, C., S. Di Lorenzo, G. Failla, and A. Pirrotta. On the moving load problem in beam structures equipped with tuned mass dampers. *Meccanica*, 52(13): 3101–3115, 2017.

Bilello, C., M. Di Paola, and A. Pirrotta. Time delay induced effects on control of non-linear systems under random excitation. *Meccanica*, 37(1–2): 207–220, 2002.

Biondi, B. and S. Caddemi. Euler–Bernoulli beams with multiple singularities in the flexural stiffness. *European Journal of Mechanics - A/Solids*, (26) 5: 789–809, 2007.

Bucher, C. and M. Di Paola. Efficient solution of the first passage problem by Path Integration for normal and Poissonian white noise. *Probabilistic Engineering Mechanics*, 41: 121–128, 2015.

Di Lorenzo, S., M. Di Paola, G. Failla, and A. Pirrotta. On the moving load problem in Euler–Bernoulli uniform beams with viscoelastic supports and joints. *Acta Mechanica*, 228(3): 805–821, 2017.

Di Matteo, A., I. P. Dunn, G. Failla, and A. Pirrotta. A novel solution to find the dynamic response of an Euler-Bernoulli beam fitted with intraspan TMDs under Poisson type loading. *Infrastructures*, 5(5), 2020.

Di Matteo, A., M. Di Paola, and A. Pirrotta. Path integral solution for nonlinear systems under parametric Poissonian white noise input. *Probabilistic Engineering Mechanics*, 44: 89–98, 2016.

Di Paola, M. and A. Pirrotta. Non-linear systems under impulsive parametric input. *International Journal of Non-Linear Mechanics*, 34(5): 843–851, 1999.

Di Paola, M. and G. Ricciardi. Vibration of a bridge under a random train of moving loads. In *Probabilistic Mechanics and Structural and Geotechnical Reliability, Proceedings of the Specialty Conference*, 136–139, 1992.

Di Paola, M., G. Falsone, and A. Pirrotta. Stochastic response analysis of nonlinear systems under Gaussian inputs. *Probabilistic Engineering Mechanics*, 7(1): 15–21, 1992.

Di Paola, M., G. Ricciardi, and M. Vasta. A method for the probabilistic analysis of nonlinear systems. *Probabilistic Engineering Mechanics*, 10(1): 1–10, 1995.

Dunn, I., A. Di Matteo, G. Failla, A. Pirrotta, and A. F. Russillo. Stochastic response of beams equipped with tuned mass dampers subjected to Poissonian loads. In Proceedings of the *13th International Conference on Applications of Statistics and Probability in Civil Engineering, ICASP*, 2019.

Failla, G. An exact generalised function approach to frequency response analysis of beams and plane frames with the inclusion of viscoelastic damping. *Journal of Sound and Vibration*, 360: 171–202, 2016.

Failla, G. On the dynamics of viscoelastic discontinuous beams. *Mechanics Research Communications*, 60: 52–63, 2014.

Failla, G., M. Di Paola, A. Pirrotta, A. Burlon, and I. Dunn. Random vibration mitigation of beams via tuned mass dampers with spring inertia effects. *Meccanica*, 54(9): 1365–1383, 2019.

Falsone, G. The Use of Generalised Functions in the Discontinuous Beam Bending Differential Equations. *International Journal of Engineering Education*, 18(3): 337-343, 2002.

Furtmüller, T., A. Di Matteo, C. Adam, and A. Pirrotta. Base-isolated structure equipped with tuned liquid column damper: An experimental study. *Mechanical Systems and Signal Processing*, 116: 816–831, 2019.

Oliveto, G., A. Santini, and E. Tripodi. Complex Modal Analysis Of A Flexural Vibrating Beam With Viscous End Conditions. *Journal of Sound and Vibration*, 200(3): 327–345, 1997.

Pirrotta, A. Non-linear systems under parametric white noise input: Digital simulation and response. *International Journal of Non-Linear Mechanics*, 40(8): 1088–1101, 2005.

Ricciardi, G. Random Vibration of Beam under Moving Loads. *Journal of Engineering Mechanics*, 120(11): 2361–2380, 1994.